LA-UR- 09-06127

Approved for public release;
distribution is unlimited.

Title:	Active Terahertz Metamaterials
Author(s):	Hou-Tong Chen John F. O'Hara Antoinette J. Taylor
Intended for:	Optics and Spectroscopy

Los Alamos
NATIONAL LABORATORY
EST. 1943

Form 836 (7/06)

ACTIVE TERAHERTZ METAMATERIALS

Hou-Tong Chen*, John F. O'Hara, and Antoinette J. Taylor

MPA-CINT, MS K771, Los Alamos National Laboratory, Los Alamos, NM 87544, USA

* E-mail: chenht@lanl.gov

Abstract

In this paper we present an overview of research in our group in terahertz (THz) metamaterials and their applications. We have developed a series of planar metamaterials operating at THz frequencies, all of which exhibit a strong resonant response. By incorporating natural materials, e.g. semiconductors, as the substrates or as critical regions of metamaterial elements, we are able to effectively control the metamaterial resonance by the application of external stimuli, e.g., photoexcitation and electrical bias. Such actively controllable metamaterials provide novel functionalities for solid-state device applications with unprecedented performance, such as THz spectroscopy, imaging, and many others.

1. Introduction

Metamaterials have been developed during the recent years as artificially structured effective media through a bottom-up approach with specifically designed subwavelength unit cells. They exhibit unusual electromagnetic or optical

properties that are very difficult or impossible to realize using naturally existing materials. Particularly, metamaterials can reveal simultaneously negative effective permittivity and permeability, and therefore negative index of refraction [1,2,3,4,5], the properties of "substances" that Veselago envisioned 40 years ago [6]. Exotic properties were predicted and now many of them have been experimentally verified. Thanks to the pioneering works by Pendry and Smith and their colleagues [1,2,7,8,9], worldwide interest continues to grow in metamaterials and has resulted in the emergence of new phenomenology and novel metamaterial structures operating over many decades of the electromagnetic spectrum [3,4,5]. Phenomena such as negative index of reflection [1,2], super-resolution in optical imaging [10,11], electromagnetic invisibility [12], and enhanced terahertz (THz) functionalities [13,14,15,16,17] are of particular interest and importance.

However, metamaterials are still in their infancy, so the ultimate real world applications still require much development and may be hard to predict. In the microwave, infrared and visible regimes, many technologies have already matured and are routinely used in our daily life. Metamaterials may have particular benefit, however, in the THz frequency range, which is loosely defined between 0.1 and 10 THz and is among the least developed regimes in the electromagnetic spectrum. THz radiation is attractive and promising for numerous applications including molecular identification and sensing, material characterization, nondestructive

detection, spectroscopy, biomedical imaging, and secure short-range wireless communication. However, at THz frequencies, both the materials' classical electronic response and the quantum photonic response die off. The resulting "THz gap" is due to the absence of materials with desirable THz response, and the consequent lack of high power compact THz sources, sensitive THz detectors, and many general THz system components such as filters, lenses, switches/modulators, phase shifters, and beam steering devices. Worldwide efforts continue in this field, but progress has been relatively slow because of the very limited number of useful natural materials.

The emergence of metamaterials with engineered and controllable properties provides unique opportunities that may have the potential to overcome these material issues and bridge the THz gap. In this paper, we present an overview of some of the most important demonstrations in our group during the past few years in the area of actively or dynamically controllable THz planar metamaterials and metamaterial-based THz devices and components.

2. Complementary Planar THz Electric Metamaterials

Split-ring resonators (SRRs) [9] having an artificially designed magnetic resonant response have played the most important role in the development of metamaterials. Three dimensional bulk metamaterials consisting of periodically arranged subwavelength SRRs and other metamaterial elements are usually

required to be considered as effective media. For certain applications, however, two-dimensional planar metamaterials are sufficient and greatly ease fabrication difficulties, particularly at THz and higher frequencies. We have designed, modeled, fabricated and characterized a series of THz planar metamaterial structures [18], termed electric SRRs with the unit cells shown in Fig. 1(a). These highly symmetric structures consist of a class of subwavelength elements that exhibit a resonant response to the electric field while minimizing or eliminating any response to the magnetic field [19]. We also fabricated and characterized their inversed metamaterial structures termed complementary metamaterials in contrast to the original metamaterials, both of which exhibit electric resonances [18]. The important difference between original and complementary metamaterials is the inversed regions of metallized and bare patterning. Both the original structures and their complements were fabricated as square planar arrays on semi-insulating gallium arsenide (SI-GaAs) substrates through conventional photolithographic methods and a lift-off process. The metamaterial samples were then characterized by transmission measurements using THz time-domain spectroscopy (THz-TDS) with a bare GaAs wafer as the reference.

The frequency dependent THz transmission amplitude spectra with normal incidence are shown in Fig. 1(b). The low frequency resonant response (<1 THz) originates from the electrically excited circulating currents in the ring (anti-ring)

structures and results in a pure electric response. All original metamaterials show a sharp resonant transmission minimum as low as 10% at frequencies between 0.5 THz and 1.0 THz. The complementary metamaterials, on the other hand, show a resonant enhanced transmission as high as 90% at the same frequencies as the transmission dips in the original metamaterials. Furthermore, the THz transmission amplitude spectra of the original and complementary metamaterials are complementary to each other [18], in accordance with the Babinet's principle. The second transmission minimum (original metamaterials) or maximum (complementary metamaterials) originates from the excitation of collective electric dipoles similar to that in cut wires or their complements.

These metamaterials may be of particular interest in applications such as far-infrared spectroscopy, astronomy, laser cavity output couplers, and Fabry-Perot interferometers. We have further designed and characterized additional metamaterial elements including rectangular SRRs controlling the coupling between fundamental and higher-order resonances [20], and elliptical SRRs showing anisotropic properties for polarimetric applications [21]. All of these planar metamaterials have founded the basis in our discovery of more advanced THz metamaterials and devices.

3. Ultrafast Dynamical Switching of Metamaterial Resonance

Although the metamaterial resonant response is mainly determined by the geometry and dimensions of the metamaterial elements, incorporation of additional materials, e.g. semiconductors, as the substrate or as an integral part of the metamaterial particles, can enable the dynamical or active control over the metamaterial response and therefore produce novel functionalities. For example, SRR arrays fabricated on high resistivity GaAs semiconductor substrate reveal very strong resonances [18]. However, under photoexcitation using near-infrared laser pulses, Padilla *et al.* demonstrated that the generated photocarriers on the substrate surface create a conducting channel that short-circuits the split gaps, which dynamically deactivates the metamaterial resonance and thereby tunes the values of the effective permittivity and/or permeability [13]. Consequently, the transmission amplitude of the THz radiation was also switched/modulated over a narrow frequency range centered at the resonance.

The advantage of this optical tuning approach is the possibility of extremely fast switching using femtosecond optical pulses. In this case, although the switching rise time is very fast, the recovery time must also be minimized to achieve fast modulation. Intrinsic GaAs has a recovery time is on the order of nanoseconds due to carrier recombination dynamics. Therefore, reducing the photocarrier lifetime is key to realizing the ultrafast switching of the metamaterial response. Various methods to shorten the carrier lifetime in semiconductors could

be employed including radiation damage and low-temperature growth to introduce defects. We used epitaxial grown GaAs:ErAs nanoisland superlattices as the metamaterial substrate, where the carrier lifetime is strongly correlated with the superlattice period L and can be engineered from sub-picosecond to tens of picoseconds [22]. In this work a 20 period GaAs:ErAs superlattice with L=100 nm resulted in a carrier lifetime of approximately 10 ps [23].

We fabricated metamaterial samples on a GaAs:ErAs substrate and characterized them using an optical-pump THz-probe system. The femtosecond near-infrared laser pulses were used to excite free charge carriers in the GaAs:ErAs substrates. At various time delays between the arrival of the synchronized THz pulses and the optical excitation, the transmitted THz field through the metamaterial sample was measured, using a bare GaAs:ErAs substrate as the reference under no photoexcitation. The experimental results are shown in Fig. 2. A strong resonant transmission dip occurs at 0.7 THz without photoexcitation. Photoexcitation of carriers in the substrates shunts the resonance, thereby increasing the transmission intensity. The resonant transmission is completely turned off within 2 ps following the photoexcitation. As the photoexcited carriers are trapped and recombine, the resonant transmission characteristics reappear, and nearly complete recovery of the metamaterial resonance is achieved within 20 ps. A complementary metamaterial device was also fabricated and characterized,

which reveals similar switching characteristics [23]. As a device, this metamaterial enables dynamical modulation of THz transmission with very high switching contrast and speed, and requires very low photoexcitation fluence.

4. Frequency Agile THz Metamaterials

The resonant nature of metamaterials results in high frequency dispersion and narrow bandwidth where the center frequency is fixed by the geometry and dimensions of the SRR elements. The creation of frequency agile metamaterials would extend the spectral range over which devices function. The metamaterial resonance frequency is determined by $\omega_0 = 2\pi(LC)^{-1/2}$, where L is the effective inductance of the SRRs and C is the effective capacitance. Therefore, tuning the metamaterial resonance frequency can be caused by altering the capacitance and/or inductance of the SRRs. We achieved such tunability through photoexcitation of semiconductors located at specific regions of metallic SRRs [15].

Fig. 3(a) shows a scanning electron microscopy (SEM) image of the unit cell of the frequency agile THz metamaterial. The gold SRR array was first fabricated on a silicon-on-sapphire (SOS) substrate with the silicon layer thickness of 600 nm and a resistivity larger than 100 Ω-cm^{-1}, through conventional photolithographic methods and lift-off processing. Silicon "capacitor plates" were formed at SRR gaps through reactive ion etching (RIE). By constructing the capacitor plates from silicon, we can control their conductivity via photoexcitation of free charge carriers.

As the plates transition from insulator to conductor they change the effective SRR capacitance C, which results in a shift of the metamaterial resonant frequency.

The metamaterial was characterized using the optical-pump THz-probe experimental system at various photoexcitation powers. The experimental results are shown in Fig. 3(b). Without photoexcitation, the metamaterial exhibits a deep resonant transmission dip at 1.06 THz having a transmission minimum of 19%. As the photoexcitation power increases, the resonance initially weakens and broadens rather than shifting the resonant frequency. In this case the small silicon conductivity induced by photoexcitation only contributes to an increased damping loss of the metamaterial resonance. Increasing the excitation power and therefore increasing the silicon conductivity results in growing contribution to the gap capacitance, and now the weakened resonance begins to shift to significantly lower frequencies. Further increases in excitation power cause continued shifting to lower frequencies and also re-establish the resonance strength and narrow the line width, because the high silicon conductivity starts to reduce the loss. The results show a tuning range of 20% in the resonance frequency. We further carried out numerical simulation by varying the silicon conductivity [15], the results of which were in excellent agreement with the experimental observations.

5. Active THz Metamaterials and Devices

It is also attractive and practical to have an electrical approach to control the metamaterial response, obviating the need for laser photoexcitation. In many THz applications, high speed electrical modulation of THz waves is highly desirable but not available. The resonant response of metamaterials dramatically enhances their interaction with THz radiation, and the resonance is very sensitive to the embedded environments of the resonators; therefore it provides new opportunities in the control and manipulation of THz waves. Our approach to accomplish electrically switchable metamaterials is to fabricate gold SRR array on a thin n-doped GaAs layer on an intrinsic GaAs substrate [14,16]. The interface of the metal resonators and the substrate forms a Schottky diode structure, where a reverse voltage bias could actively deplete free electrons in the substrate under the resonator split gaps, thereby electrically tuning the metamaterial resonant response. Consequently, the THz transmission is actively switched and modulated.

Fig. 4(a) shows one unit cell of our designs for such electrically switchable metamaterial devices. The transmission amplitude and phase spectra under various reverse voltage biases are shown in Fig. 4(b) and (c), respectively. Under no voltage bias, the metamaterial resonance is significantly weakened due to the fact that the conducting substrate surface, particularly near the split gaps, damps the resonance. Application of a reverse voltage bias depletes the electrons away from the substrate surface and reduces the gap conductivity and loss, thus re-establishing

the metamaterial resonance. At a relatively low voltage bias of 16 volts, the amplitude of the resonant transmitted terahertz electric field has decreased from t_{0V} = 0.56 to t_{16V} = 0.25, a change (or modulation depth) of 55% (transmission power change of 80%), as shown in Fig. 4(b). The transmission amplitude at of the second resonance at 1.7 THz has decreased from t_{0V} = 0.48 to t_{16V} = 0.30; the switching performance is less efficient than the lower frequency fundamental resonance. Between the two resonances the reverse voltage bias significantly increases the THz transmission amplitude. The modulation depth is about a 20-fold improvement over the earlier electrically driven THz modulator based on semiconductor quantum well structures [24], and the metamaterial devices operate at room temperature, without the need of cryogenic cooling [25,26]. Its modulation speed is also far higher than electrical THz modulators based on liquid crystals [27].

In addition to switching of THz transmission amplitude, its phase also varies as a function of the applied voltage bias, as shown in Fig. 4(c). The phase of the THz transmission is ϕ_{16V} = -0.51 rad under the reverse voltage bias of 16 volts as compared to ϕ_{0V} = 0.05 with no voltage bias, a shift of $\Delta\phi = \pi/6$ for a single planar metamaterial layer, which makes it an efficient solid-state THz phase modulator [16]. It was found that the amplitude switching and phase shifting both have a linear dependence on the voltage bias [16]. In such a way, the effective permittivity

in electric metamaterials can be conveniently and effectively tuned, because it is directly related to the phase shifting [15].

From the results shown in Fig. 4(b) and (c) it was found that the amplitude switching and phase shifting as a function of voltage bias are correlated through the Kramers-Kronig (KK) relations. Near frequencies where the amplitude is not strongly dependent on the applied bias voltage, but its slope is, the phase experiences a maximum shift, and vice versa. Thus, although the amplitude modulation and phase shifting are inherently narrowband phenomena associated with the resonant nature of metamaterials, the total THz modulation signal when applying an ac voltage bias is given by

$$\Delta\tilde{t}(\omega) = \left| t_{V1}(\omega) e^{i\phi_{V1}(\omega)} - t_{V2}(\omega) e^{i\phi_{V2}(\omega)} \right|, \qquad (1)$$

which shows that both the amplitude and phase contribute to the THz modulation signal, making the device capable of a broadband modulation in THz-TDS [16].

Fig. 5(a) shows the experimental results of the metamaterial device acting as a broadband modulator. The THz time-domain waveform of the modulation (differential) signal was obtained by application of a square-wave voltage bias to the metamaterial and alternating between 0 and 16 V. As a reference, the THz transmission signal through a bare GaAs substrate was also measured using an optical chopper. The normalized THz modulation spectrum produced by the metamaterial device is shown in Fig. 5(b) and displays a broadband and rather flat

response of between 0.8 and 1.7 THz, roughly between the two metamaterial resonant frequencies, beyond which the THz radiation is also modulated but with decreasing modulation depth. By using rectangular electric SRR designs the modulation bandwidth can cover the whole THz band of interest [20]. We have successfully applied this integrable THz broadband modulator in THz time-domain spectroscopy measurements, replacing the bulky low speed mechanical optical chopper. It allows for similar modulation performance in the THz-TDS measurements [16] but is capable of higher modulation speeds of up to 2 MHz limited only by the device parasitic capacitance [28]. Much higher modulation speeds are theoretically realizable. Additionally, we demonstrated that our active THz metamaterials are capable of modulating THz laser emission from a THz quantum cascade laser, and we also fabricated a metamaterial device with independently controllable pixels to demonstrate a spatial light modulator for THz imaging applications [29].

6. Conclusions

The above examples clearly show that dynamically or actively controlling metamaterial resonant properties has the potential to solve some material issues associated with the THz gap. Metamaterials provide novel functionalities for THz applications, which are not easily found in natural materials. The demonstrations we have shown suggest that metamaterials will definitely play an increasingly

important role in THz technology. Further investigations include but are not limited to metamaterial antireflection coatings for impedance matching (i.e. reducing insertion loss), and combining metamaterials with nonlinearities, which we expect will elicit numerous exciting discoveries. With certain limitations, our demonstrations at THz frequencies could be extended to other frequency regimes as well.

Acknowledgements

We acknowledge support from the Los Alamos National Laboratory LDRD Program. This work was performed, in part, at the Center for Integrated Nanotechnologies, a US Department of Energy, Office of Basic Energy Sciences Nanoscale Science Research Center operated jointly by Los Alamos and Sandia National Laboratories. Los Alamos National Laboratory, an affirmative action/equal opportunity employer, is operated by Los Alamos National Security, LLC, for the National Nuclear Security Administration of the US Department of Energy under contract DE-AC52-06NA25396.

References:

[1] D. R. Smith, W. J. Padilla, D. C. Vier, S. C. Nemat-Nasser, and S. Schultz, *Phys. Rev. Lett.* **84**, 4184 (2000).

[2] R. A. Shelby, D. R. Smith, and S. Schultz, *Science* **292**, 77 (2001).

[3] W. J. Padilla, D. N. Basov, and D. R. Smith, *Mater. Today* **9**, No. 7-8, 28 (2006).

[4] C. M. Soukoulis, M. Kafesaki, and E. N. Economou, *Adv. Mater.* **18**, 1941 (2006).

[5] V. M. Shalaev, *Nature Photon.* **1**, 41 (2007).

[6] V. G. Veselago, *Sov. Phys. Usp.* **10**, 509-514 (1968).

[7] J. B. Pendry, *Phys. Rev. Lett.* **85**, 3966 (2000).

[8] J. B. Pendry, A. J. Holden, W. J. Stewart, and I. Youngs, *Phys. Rev. Lett.* **76**, 4773 (1996).

[9] J. B. Pendry, A. J. Holden, D. J. Robbins, and W. J. Stewart, *IEEE Trans. Microwave Theory and Tech.* **47**, 2075 (1999).

[10] D. O. S. Melville and R. J. Blaikie, *Opt. Express* **13**, 2127 (2005).

[11] N. Fang, H. Lee, C. Sun, and X. Zhang, *Science* **308**, 534 (2005).

[12] D. Schurig, J. J. Mock, B. J. Justice, S. A. Cummer, J. B. Pendry, A. F. Starr, and D. R. Smith, *Science* **314**, 977 (2006).

[13] W. J. Padilla, A. J. Taylor, C. Highstrete, M. Lee, and R. D. Averitt, *Phys. Rev. Lett.* **96**, 107401 (2006).

[14] H.-T. Chen, W. J. Padilla, J. M. O. Zide, A. C. Gossard, A. J. Taylor, and R. D. Averitt, *Nature* **444**, 597 (2006).

[15] H.-T. Chen, J. F. O'Hara, A. K. Azad, A. J. Taylor, R. D. Averitt, D. B. Shrekenhamer, and W. J. Padilla, *Nature Photon.* **2**, 295 (2008).

[16] H.-T. Chen, W. J. Padilla, M. J. Cich, A. K. Azad, R. D. Averitt, and A. J. Taylor, *Nature Photon.* **3**, 148 (2009).

[17] W. Withayachumnankul and D. Abbott, *IEEE Photonics. J* **1**, 99 (2009).

[18] H.-T. Chen, J. F. O'Hara, A. J. Taylor, R. D. Averitt, C. Highstrete, M. Lee, and W. J. Padilla, *Opt. Express* **15**, 1084 (2007).

[19] W. J. Padilla, *Opt. Express* **15**, 1639 (2007).

[20] J. F. O'Hara, A. K. Azad, H.-T. Chen, A. J. Taylor, and E. Smirnova, *Active and Passive Electronic Components*, Vol. **2007**, Article ID 49691, doi: 10.1155/2007/49691 (2007).

[21] X. G. Peralta, E. I. Smirnova, A. K. Azad, H.-T. Chen, A. J. Taylor, I. Brener, and J. F. O'Hara, *Opt. Express* **17**, 773 (2009).

[22] C. Kadow, S. B. Fleischer, J. P. Ibbetson, J. E. Bowers, A. C. Gossard, J. W. Dong, and C. J. Palmstrøm, Appl. Phys. Lett. **75**, 3548 (1999).

[23] H.-T. Chen, W. J. Padilla, J. M. O. Zide, S. R. Bank, A. C. Gossard, A. J. Taylor, and R. D. Averitt, *Opt. Lett.* **32**, 1620 (2007).

[24] T. Kleine-Ostmann, P. Dauson, K. Pierz, G. Hein, and M. Koch, *Appl. Phys. Lett.* **84**, 3555 (2004).

[25] R. Kersting, G. Strasser, and K. Unterrainer, *Electron. Lett.* **36**, 1156 (2000).

[26] I. H. Libon, S. Baumgärtner, M. Hempel, N. E. Hecker, J. Feldmann, M. Koch, and P. Dawson, *Appl. Phys. Lett.* **76**, 2821 (2000).

[27] C.-F. Hsieh, R.-P. Pan, T.-T. Tang, H.-L. Chen, and C.-L. Pan, *Opt. Lett.* **31**, 1112 (2006).

[28] H.-T. Chen, S. Palit, T. Tyler, C. M. Bingham, J. M. O. Zide, J. F. O'Hara, D. R. Smith, A. C. Gossard, R. D. Averitt, W. J. Padilla, N. M. Jokerst, and A. J. Taylor, *Appl. Phys. Lett.* **93**, 091117 (2008).

[29] W. L. Chan, H.-T. Chen, A. J. Taylor, I. Brener, M. J. Cich, and D. M. Mittleman, *Appl. Phys. Lett.* **94**, 213511 (2009).

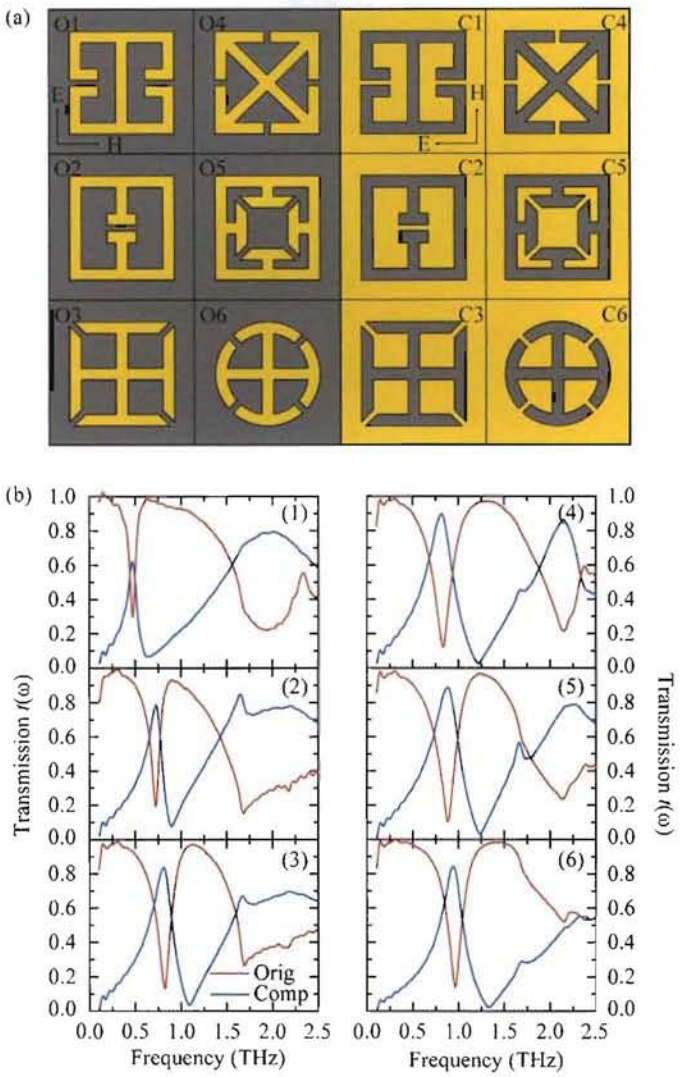

Fig. 1: (a) Schematic geometry of original (O1-O6) and complementary (C1-C6) planar metamaterial unit cells. (b) THz transmission amplitude spectra of the corresponding metamaterials. The polarization of normally incident THz radiation is configured as shown in O1 and C1 for the original and complementary metamaterials, respectively.

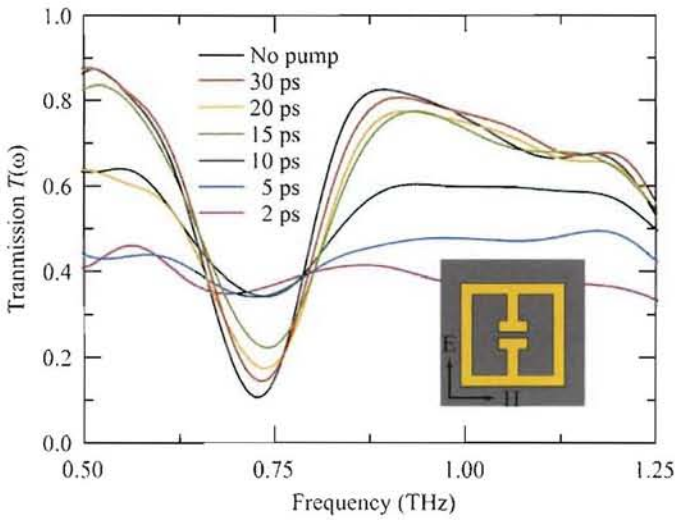

Fig. 2: THz power transmission spectra through the metamaterial sample at various time delays of THz pulse following the photoexcitation. Inset, metamaterial eSRR unit cell; arrows, polarization of the normally incident THz radiation.

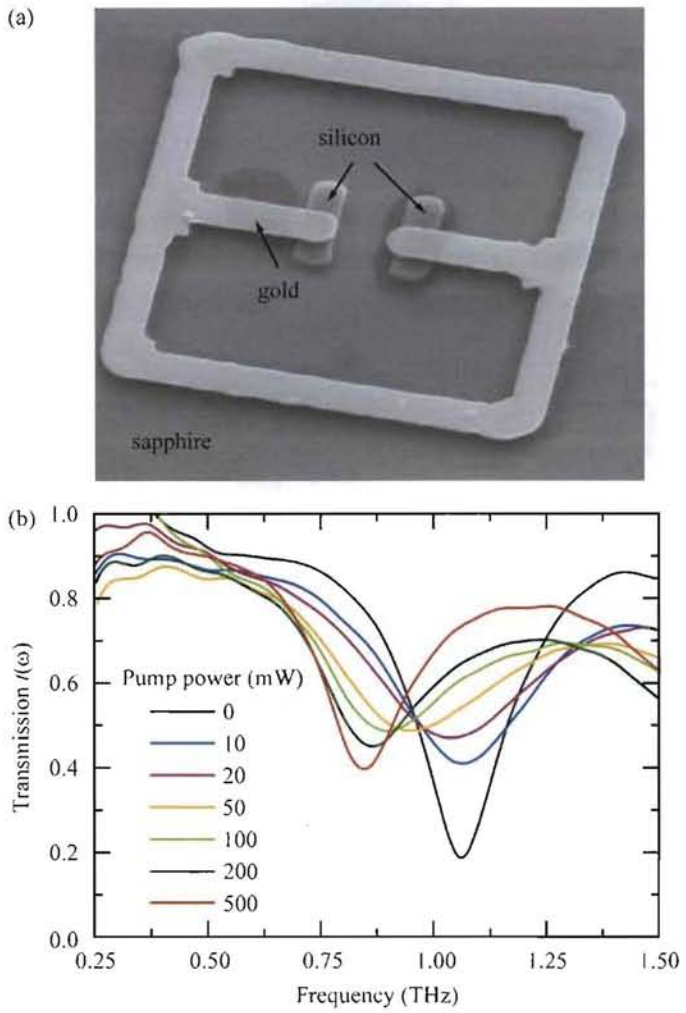

Fig. 3: (a) Scanning electron microscopy image of an individual unit cell of the frequency agile planar metamaterial. (b) Experimental THz transmission amplitude spectra as a function of photoexcitation power.

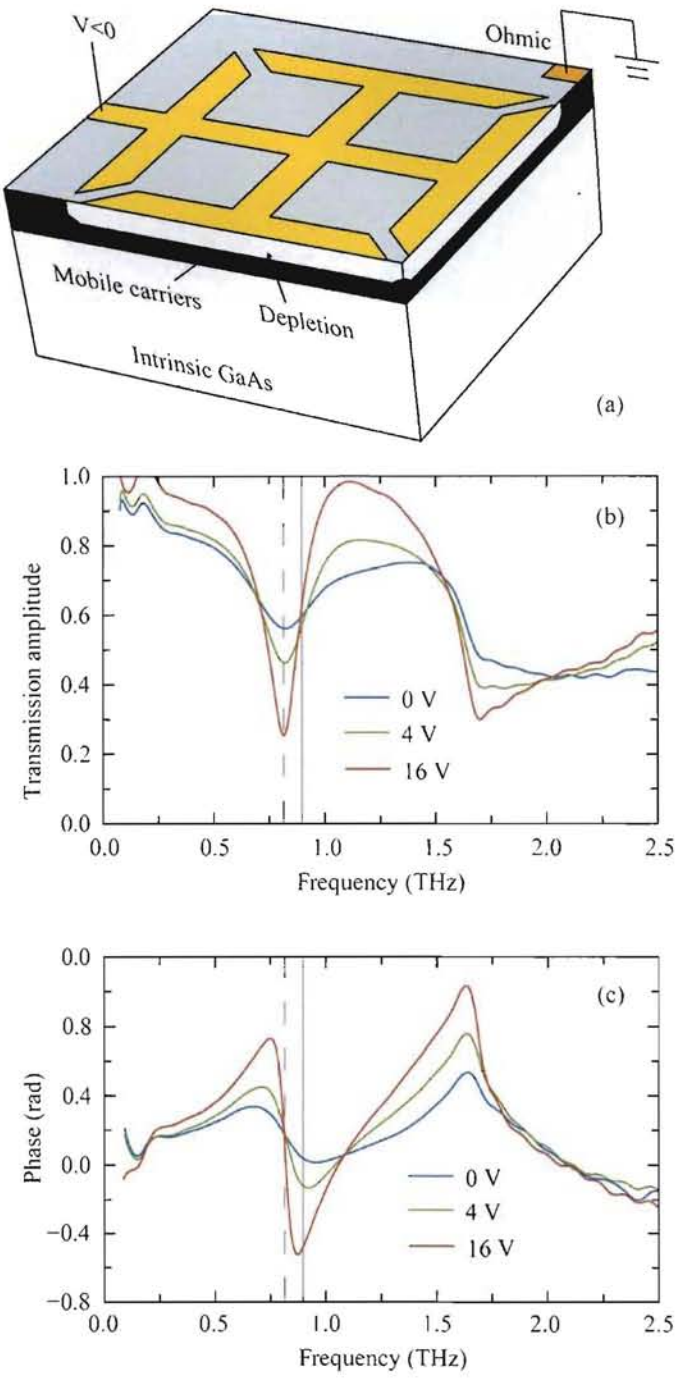

Fig. 4: (a) Schematic design of the unit cell of an electrically switchable metamaterial device. (b) THz transmission amplitude and (c) phase spectra through the metamaterial device under several reverse voltage biases.

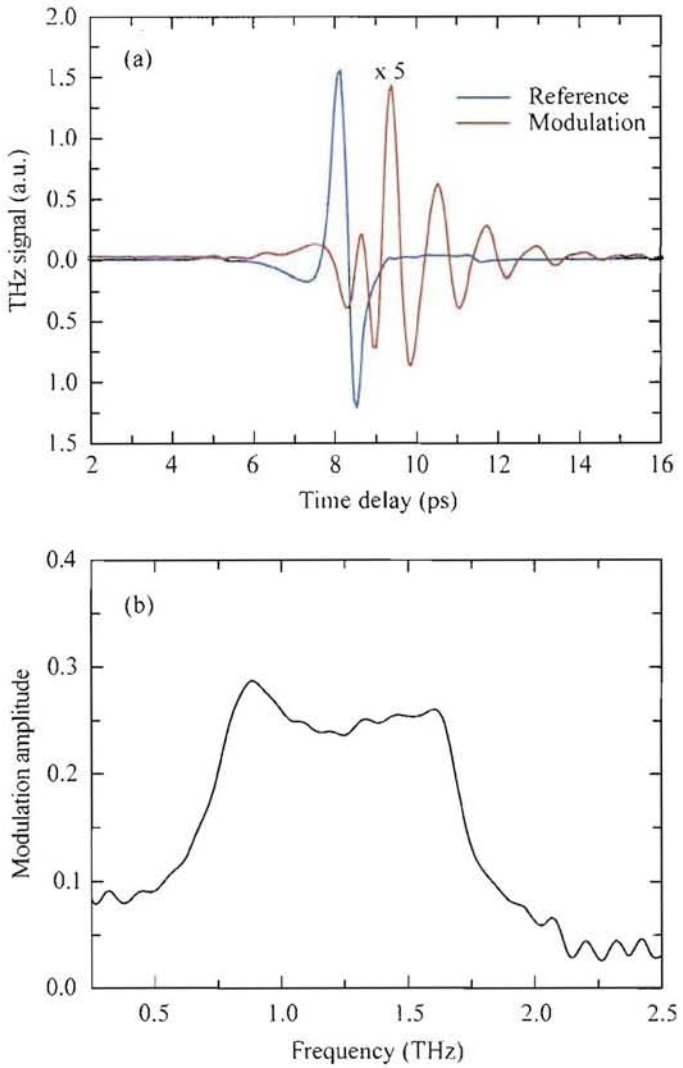

Fig. 5: (a) Time-domain measurements of the THz modulation (differential) signal with a square-wave voltage bias applied to the metamaterial device and alternating between 0 and 16 V. The reference THz signal was measured through a bare GaAs substrate using a mechanical chopper. (b) The amplitude spectrum of the complex modulation normalized by the reference.